


**Anisotropy-exchange resonance as a mechanism for entangled state switching**Eric D. Switzer <sup>1</sup>, Xiao-Guang Zhang <sup>2</sup> and Talat S. Rahman <sup>1,\*</sup><sup>1</sup>*Department of Physics, University of Central Florida, Orlando, Florida 32816, USA*<sup>2</sup>*Department of Physics, Center for Molecular Magnetic Quantum Materials and Quantum Theory Project, University of Florida, Gainesville, Florida 32611, USA* (Received 2 May 2021; revised 15 October 2021; accepted 11 November 2021; published 30 November 2021)

We explore the three-particle spin model of an  $S_1 = \frac{1}{2}$  particle (e.g., an electron) interacting with two spin-coupled  $S_{2,3}$  particles with exchange coupling and magnetic anisotropy. We show that in the case of  $S_{2,3} = 1$  particles, the coupled particle entanglement states can be prepared, controlled, and read by the  $S_1$  particle. We also find that for particular resonance conditions of the magnetic anisotropy strength  $D$  and exchange coupling strength  $J$ , the entanglement state-switching behavior is maximized and is robust against a range of anisotropic application of the exchange coupling.

DOI: [10.1103/PhysRevA.104.052434](https://doi.org/10.1103/PhysRevA.104.052434)**I. INTRODUCTION**

Spin state entanglement plays a key role in many systems, including those considered within quantum information science (QIS). For example, spin qubits, the coherent superposition of spin states within quantum objects, make use of entangled spin states for quantum gate operations [1]. Spin qubits have been explored theoretically and experimentally, notably in the application of confined electrons in quantum dots fabricated in semiconductors [2–9] and the search for robust QIS-applicable magnetic molecule systems [10–17]. Molecular magnets in particular possess an onsite magnetic anisotropy which gives rise to their unique magnetic properties. Molecular magnets are viable candidates for spin state switching for QIS purposes because of their long coherence times, the ability to tunnel between spin states resulting from their magnetic anisotropy, and tailorable ligands [18]. For example, the single-molecule magnet  $\text{TbPc}_2$  possesses a nuclear spin that is electrically controllable and has long coherence times [15,17]. In both of these QIS approaches, the Kondo effect has been found [19–21], and thus the Kondo or Anderson impurity model [22,23] is applicable to predict some of the features of these systems.

With these considerations, a QIS system that contains onsite magnetic anisotropy is expected to have a complex interaction between the system's anisotropy and effective exchange coupling. While some studies have examined the interplay of exchange coupling and onsite magnetic anisotropy for two particles [24], the three-particle case is a qualitatively different system that has not been fully explored. Some experimental and theoretical studies have realized multiple-quantum dot scenarios [5–7,25] or studied the two magnetic impurity entanglement state dependency of contact exchange interactions with incident electrons [26–28]. As described in the effectively three-spin-particle setup in Ref. [29], the strong-coupling Kondo exchange regime and

the weak-coupling spin-orbit interaction regime compete with each other, resulting in a nontrivial interaction. Outside of QIS, a similar balance between exchange coupling and magnetic anisotropy has been recently found experimentally in a Mott insulator composed of an ultracold optical lattice of  $^{87}\text{Rb}$  atoms [30]. In all of these studies, the exchange coupling mechanism plays a significant role in controlling the system of interest. Unintended variations in this exchange can cause undesirable effects, and thus a system must be correspondingly robust against them.

In this work, we explore a general spin model with exchange and magnetic anisotropy that encompasses these scenarios and investigates the robustness of the spin system by extending the two-particle case of Ref. [24] to the three-particle paradigm. We consider two magnetic sites of either  $S_{2,3} = \frac{1}{2}$  or  $S_{2,3} = 1$  in which an exchange interaction is applied either isotropically or anisotropically between them and the  $S_1 = \frac{1}{2}$  particle. Because we do not treat the electronic degrees of freedom and instead focus solely on the model's spin degrees of freedom, our model is a general one with physical analogs in the recently realized experiments of three quantum dots [5–7] and ultracold optical lattices [30]. As we will show, we find that for the  $\text{C}^{18}$  state space model corresponding to  $S_{2,3} = 1$ , the exchange and anisotropy interactions lead to a set of necessary conditions on the exchange and magnetic anisotropy strengths that correspond with perfect nonentangled to entangled state switching in four smaller  $\text{SO}(2)$  representation subgroups. We find that at these special resonance conditions, which we designate as “ $D$ - $J$  resonances,” measurement of the coupled particle entanglement states is possible by measurement of the  $S_1 = \frac{1}{2}$  particle's spin. We also show the conditions in which these  $D$ - $J$  resonances allow for complete control of appropriately chosen Bloch vectors within a subspace of the coupled particles' total spin space, which is not found for the  $S_{2,3} = \frac{1}{2}$  model. We demonstrate conditions for full control of this Bloch vector, and that for a relevant molecular magnet example, state coherence is robust against anisotropic application of the exchange coupling.

\*Corresponding author: [talat.rahman@ucf.edu](mailto:talat.rahman@ucf.edu)

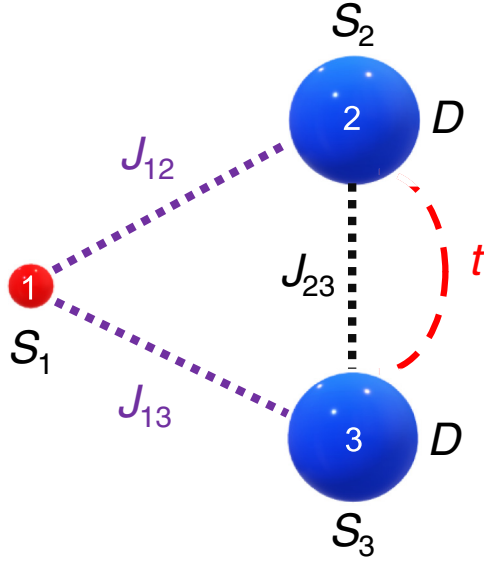


FIG. 1. Schematic of the spin model considered in this work. Particles 2 and 3 are coupled by an exchange interaction  $J_{23}$ . Particle 1 is also coupled to particles 2 and 3 by an exchange interaction,  $J_{12}$  and  $J_{13}$ , respectively. Particle 1 is allowed to hop between particle 2 and particle 3 with hopping strength  $t$ .

## II. THREE-PARTICLE SPIN MODEL

A representative schematic of the resulting spin model is shown in Fig. 1. The spin Hamiltonian ( $\hbar = 1$ ) is then

$$\mathcal{H} = \mathcal{H}_{12} + \mathcal{H}_{13} + \mathcal{H}_{23} + \mathcal{H}_A + \mathcal{H}_t, \quad (1)$$

where each term in the Hamiltonian is explained as follows. Motivated by the application of exchange coupling between two coupled dimers [31], the exchange interaction of the two  $S_{2,3}$  particles is represented by

$$\mathcal{H}_{23} = J_z \hat{S}_2^z \hat{S}_3^z + J_{xy} (\hat{S}_2^x \hat{S}_3^x + \hat{S}_2^y \hat{S}_3^y), \quad (2)$$

where  $\hat{\mathbf{S}}_i = (\hat{S}_i^x, \hat{S}_i^y, \hat{S}_i^z)$  is the spin operator for the  $i$ th particle,  $J_z$  is the strength of the exchange interaction between particles 2 and 3 parallel to the direction of the magnetic anisotropy axis, and  $J_{xy}$  is the strength of the exchange interaction between particles 2 and 3 perpendicular to the direction of the magnetic anisotropy axis. When this interaction is taken to be isotropic, i.e.,  $J_z = J_{xy} \equiv J_{23}$ , this equation simplifies to  $\mathcal{H}_{23} = J_{23} \hat{\mathbf{S}}_2 \cdot \hat{\mathbf{S}}_3$ . The interaction of the  $S_1 = \frac{1}{2}$  particle with the  $S_{2,3}$  particles is closely related to the spin portion of the Kondo interaction and may be represented by

$$\mathcal{H}_{1i} = \frac{J_{1i}}{2} \sum_{\mu, \mu'} \hat{\mathbf{S}}_i \cdot \hat{d}_{\mu, i}^\dagger \hat{\sigma}_{\mu, \mu'} \hat{d}_{\mu', i}, \quad (3)$$

where  $\mu$  is a spin index for particle 1,  $\hat{\sigma}_{\mu, \mu'}$  is the corresponding  $\mu, \mu'$  matrix element of the  $s = \frac{1}{2}$  Pauli matrix, and  $\hat{d}_{\mu, i}^\dagger / \hat{d}_{\mu, i}$  represents (in second quantization language) the creation or annihilation operator of a state in which particle 1 is bound to particle  $i$ . In our general treatment, we allow  $J_{12}$  and  $J_{13}$  to take all values, i.e., we consider both ferromagnetic and antiferromagnetic possibilities.

Additionally, we consider situations in which  $S_{2,3} = 1$  particles possess an anisotropic response to applied magnetic fields,

$$\mathcal{H}_A = D(\hat{S}_2^z \hat{S}_2^z + \hat{S}_3^z \hat{S}_3^z), \quad (4)$$

where  $D$  is a uniaxial anisotropy strength. Our general treatment permits  $D$  to span all values, which allows one to consider both “easy-axis” and “hard-axis” anisotropies. The physical origin of the magnetic anisotropy, also called “zero-field splitting,” is dependent on the manifestation of the  $S_{2,3}$  particles. For example, if the two spin particles refer to magnetic molecules, the primary source of magnetic anisotropy could be from geometric distortions (Jahn-Teller distortions) of constituent ions [32]. In the ultracold optical lattice context, an effective magnetic anisotropy is created by direct on-site interactions between atoms in two states [30].

While we consider the spin interactions of three particles in this work, one can in principle pursue a more realistic treatment of the three-particle problem by incorporating the spatial degrees of freedom. If one were to extend our model spatially, the movement of the particles will impact the time-dependent dynamics of the system nontrivially. The purpose of this work, however, is to elucidate the spin dynamics of the three-particle model, which may serve as a necessary, but not sufficient, picture on realizing useful control of the system’s spin states. We balance these considerations by accommodating for Hamiltonian terms that may not play a key role in spin dynamics, but ultimately may be pivotal in more realistic contexts. In this light, we follow in the footsteps of other models (such as the Hubbard model) and include a term that describes the movement of the  $S_1$  particle hopping from the  $S_2$  particle to  $S_3$  and vice versa. In spin space, this hopping term takes the form

$$\mathcal{H}_t = \sum_{\mu} \{t \hat{d}_{\mu, 2}^\dagger \hat{d}_{\mu, 3} + \text{H.c.}\}, \quad (5)$$

where  $\mu$  is the spin index for particle 1, and  $t$  is the hopping strength.

Incorporating each of the aforementioned Hamiltonian terms, we provide a representative example of Fig. 1. One could imagine a scenario of a magnetic molecule dimer (e.g., coupled  $\text{Tb}^{\text{III}}$  ions in a molecular complex) placed on a weakly interacting substrate next to a quantum dot. Exchange interactions could then be achieved by appropriate gating. The dynamics of the system, which may involve entangled particle scenarios, is described by the density operator  $\rho$  in the Schrödinger picture,

$$i \frac{\partial \rho}{\partial t} = [\mathcal{H}, \rho], \quad (6)$$

where the brackets denote the commutator.

There are various basis sets that uncover different aspects of the dynamics of the three-spin system. One convenient representation of the Hamiltonian and density operator can be built from the basis  $|s, m_s\rangle$ , where  $\mathbf{S} = \mathbf{S}_1 + \mathbf{S}_2 + \mathbf{S}_3$ . Because we also need to examine the possible entangled states of the  $S_{2,3}$  particles in anticipation of correlating states within a qubit representation, we designate a “device” basis with states  $|s_1, m_1\rangle |s_{23}, m_{23}\rangle$ . In this representation, the  $|s_{23}, m_{23}\rangle$  states are designated the “coupled particle” basis states.

### III. RESULTS

We first consider the  $S_{2,3} = 1$  model and the impact of each term within the total Hamiltonian of Eq. (1) on the states of the system. We find that the hopping term given in Eq. (5) is diagonal in the spin space and can therefore be ignored for purposes of examining the spin dynamics of the system. We remove the hopping term in what follows, though one may not be able to ignore it when considering a spatial extension of the considered model. Next, when the exchange Hamiltonians involving  $S_1$  are applied anisotropically (i.e.,  $J_{12} \neq J_{13}$ ), the Hamiltonian connects states between different  $s_{23}$  subspaces in the device representation and can no longer be block diagonalized by the  $s_{23}$  subspaces. Instead, the effective exchange Hamiltonian can be block diagonalized by  $m$  values, where  $\mathcal{H}_m$  is the block Hamiltonian corresponding to  $m$ , and  $\mathcal{H}_{\pm 5/2}$  are diagonal. In the  $\mathcal{H}_{\pm 3/2}$  subspaces, the  $|m_1\rangle|s_{23}, m_{23}\rangle = |\pm\frac{1}{2}\rangle|2, \pm 1\rangle$ ,  $|\pm\frac{1}{2}\rangle|1, \pm 1\rangle$ , and  $|\mp\frac{1}{2}\rangle|2, \pm 2\rangle$  states participate, forming three-dimensional subspaces. Similarly, the  $\mathcal{H}_{\pm 1/2}$  subspaces contain the interactions of the  $|\pm\frac{1}{2}\rangle|2, 0\rangle$ ,  $|\pm\frac{1}{2}\rangle|1, 0\rangle$ ,  $|\pm\frac{1}{2}\rangle|0, 0\rangle$ ,  $|\mp\frac{1}{2}\rangle|2, \pm 1\rangle$ , and  $|\mp\frac{1}{2}\rangle|1, \pm 1\rangle$  states, making the subspaces five-dimensional. These forms of the effective exchange Hamiltonian will play a pivotal role in transitions between states with the same  $m$  value.

In the  $S_{2,3} = 1$  model, resonant transitions between states are found in several of the  $m$  subspaces. By inspecting the  $m = \frac{3}{2}$  subspace, which corresponds with the dynamics of the  $|m_1\rangle|s_{23}, m_{23}\rangle = \{|\uparrow\rangle|2, 1\rangle, |\uparrow\rangle|1, 1\rangle, |\downarrow\rangle|2, 2\rangle\}$  states, the block Hamiltonian takes the form (a common  $t + t^* + J_{xy} + D + \frac{1}{4}\Sigma_1$  is removed from the diagonal),

$$\mathcal{H}_{3/2} = \frac{1}{4} \begin{pmatrix} 0 & \Delta_1 & 2\Sigma_1 \\ \Delta_1 & -8J_{xy} & -2\Delta_1 \\ 2\Sigma_1 & -2\Delta_1 & -3\Sigma_1 + 4D + 4\Delta_{23} \end{pmatrix}, \quad (7)$$

where the notation  $\Delta_1 \equiv J_{12} - J_{13}$ ,  $\Sigma_1 \equiv J_{12} + J_{13} \equiv 2J_1$ , and  $\Delta_{23} \equiv J_z - J_{xy}$  has been introduced. When the application of the  $S_1$  exchange coupling is isotropic by choosing  $J_{12} = J_{13} = J_1$  and  $\Delta_1 = 0$ , the  $|\uparrow\rangle|1, 1\rangle$  state is no longer coupled to the other states within this block. Under these conditions, the total Hamiltonian takes the form

$$\mathcal{H}_{\text{eff}} = J_z \hat{S}_2^z \hat{S}_3^z + J_{xy} (\hat{S}_2^x \hat{S}_3^x + \hat{S}_2^y \hat{S}_3^y) + J_1 (\hat{\mathbf{S}}_1 \cdot \hat{\mathbf{S}}_2 + \hat{\mathbf{S}}_1 \cdot \hat{\mathbf{S}}_3) + D (\hat{S}_2^z \hat{S}_2^z + \hat{S}_3^z \hat{S}_3^z). \quad (8)$$

Inspecting the  $m = 3/2$  subspace again, the effective Hamiltonian block becomes

$$-\frac{1}{2} \left( D - \frac{3}{2} J_1 + \Delta_{23} \right) \begin{pmatrix} 1 & 0 \\ 0 & -1 \end{pmatrix} + J_1 \begin{pmatrix} 0 & 1 \\ 1 & 0 \end{pmatrix}. \quad (9)$$

For comparison, the same procedure is repeated for the  $m = 1/2$  subspace, where the effective Hamiltonian corresponding with the  $|\uparrow\rangle|1, 0\rangle$  and  $|\downarrow\rangle|1, 1\rangle$  basis takes the form

$$\frac{1}{2} \left( D + \frac{1}{2} J_1 - \Delta_{23} \right) \begin{pmatrix} 1 & 0 \\ 0 & -1 \end{pmatrix} + \frac{1}{\sqrt{2}} J_1 \begin{pmatrix} 0 & 1 \\ 1 & 0 \end{pmatrix}. \quad (10)$$

If one prepares the initial density matrix of the system to represent a pure  $|\downarrow\rangle|2, 2\rangle$  state (e.g., by utilizing a setup similar to Refs. [6,7] to prepare a particular spin state), an application of the Rabi formula results in the probability of

TABLE I. Pure state transitions for the  $S_{2,3} = 1$  model, where  $J_R$  is the condition on  $J_1$  to reach resonance,  $P_R$  is the maximum transition probability amplitude at resonance, and  $\Omega_R$  is the Rabi frequency at resonance.

State transitions	$J_R$	$P_R$	$\Omega_R$
$ \uparrow\rangle 2, +1\rangle,  \downarrow\rangle 2, +2\rangle$	$\frac{2}{3}(D + \Delta_{23})$	1	$\frac{2}{3} D + \Delta_{23} $
$ \uparrow\rangle 2, -2\rangle,  \downarrow\rangle 2, -1\rangle$	$\frac{2}{3}(D + \Delta_{23})$	1	$\frac{2}{3} D + \Delta_{23} $
$ \uparrow\rangle 1, 0\rangle,  \downarrow\rangle 1, +1\rangle$	$-2(D - \Delta_{23})$	1	$\sqrt{2} D - \Delta_{23} $
$ \uparrow\rangle 1, -1\rangle,  \downarrow\rangle 1, 0\rangle$	$-2(D - \Delta_{23})$	1	$\sqrt{2} D - \Delta_{23} $

measuring the  $|\uparrow\rangle|2, 1\rangle$  state as

$$P_{|\uparrow\rangle|2,+1\rangle}(t) = \left( \frac{J_1}{\Omega} \right)^2 \sin^2(\Omega t), \quad (11)$$

with Rabi frequency

$$\Omega = \sqrt{J_1^2 + \frac{1}{4} \left( D - \frac{3}{2} J_1 + \Delta_{23} \right)^2}. \quad (12)$$

Transforming between the considered device basis states and their site-basis representation ( $|m_1\rangle|s_{23}, m_{23}\rangle \rightarrow |m_1\rangle|m_2\rangle|m_3\rangle$ ),

$$|\downarrow\rangle|2, 2\rangle = |\downarrow\rangle|1\rangle|1\rangle, \quad (13)$$

$$|\uparrow\rangle|2, 1\rangle = \frac{1}{\sqrt{2}} (|\uparrow\rangle|0\rangle|1\rangle + |\uparrow\rangle|1\rangle|0\rangle), \quad (14)$$

one can see that the  $|\downarrow\rangle|2, 2\rangle$  state corresponds with a non-entangled coupled particle state, and the  $|\uparrow\rangle|2, 1\rangle$  corresponds with a maximally entangled coupled particle state. Thus a single measurement of particle 1's spin orientation determines the entanglement state of particles 2 and 3. This demonstrates the readout of the entanglement state if the measurement of the  $S_1$  spin polarization is taken at any general time  $t$ . This also demonstrates preparation of the entanglement state if the  $S_1$  spin polarization is measured at a specific time  $t$  corresponding with a peak in the Rabi oscillation.

As shown in Eqs. (9) and (10), the magnetic anisotropy  $D$ , average exchange interaction strength  $J_1$ , and the anisotropy of the  $S_2 - S_3$  exchange interaction  $\Delta_{23}$  determine the Rabi frequency and transition amplitudes of the system. When the Rabi frequencies and amplitudes are calculated for the other possible two state systems in the  $S_{2,3} = 1$  model, we see that particular conditions on the magnitude and sign of  $J_1$ ,  $\Delta_{23}$ , and  $D$  result in resonant transition probabilities, i.e., each state's transition probability oscillates with a maximum amplitude of 1. Table I lists these possible magnetic anisotropy and exchange strength resonance conditions, i.e.,  $D$ - $J$  resonances, for two-state switching. To see the physical consequence of these  $D$ - $J$  resonances, we turn to a representation of the states involved in a transition, where one can project the two-state systems onto a Bloch sphere. For the  $m = 3/2$  case, Eq. (9) is written suggestively to highlight the effect of the unitary operator  $U(t) = e^{-i\mathcal{H}t}$  on the Bloch vector  $\mathbf{V}$  prepared as  $(|\mathbf{V}\rangle, \theta, \phi) = (1, 0, 0)$ . In the case of Eq. (9), the Bloch vector's poles are defined by the  $|\downarrow\rangle|2, 2\rangle$  and  $|\uparrow\rangle|2, 1\rangle$  states. The first term in Eq. (9) corresponds

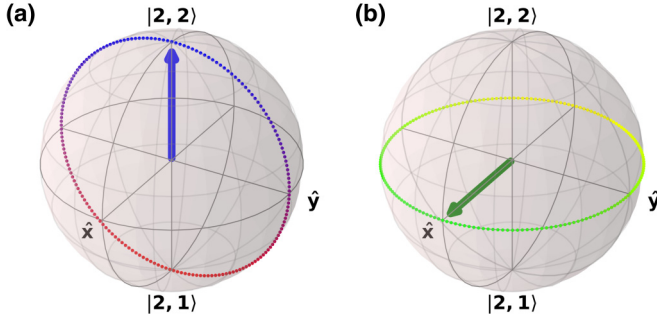


FIG. 2. Bloch sphere representation of the states within the  $|\downarrow\rangle|2, 2\rangle, |\uparrow\rangle|2, 1\rangle, m = \frac{3}{2}$  subspace when  $J_{12} = J_{13} = J_1$ . (a) When  $J_1$  is tuned to a  $D$ - $J$  resonance, rotation about the  $x$ -axis is realized. (b) When  $J_1 = 0$ ,  $(D + \Delta_{23})$ -modulated rotation about the  $z$ -axis is possible.

with a rotation (up to a global phase) of the Bloch vector about the  $z$ -axis with a frequency  $D - \frac{3}{2}J_1 + \Delta_{23}$  and the second with a rotation about the  $x$ -axis with a frequency of  $2J_1$ .

As shown in Fig. 2, at the  $D$ - $J$  resonance condition of  $J_1 = \frac{2}{3}D + \Delta_{23}$ , the  $z$ -axis rotation vector is 0, and the Bloch vector is rotated solely about the  $x$ -axis. In this way, with appropriate pulsing of the  $D$ - $J$  resonance condition, control of the Bloch vector in the  $x = 0$  plane is realized. Physically the magnitude of the exchange couplings and magnetic anisotropy determine the contribution of the device states that are energetically favorable for that parameter. At the  $D$ - $J$  resonance, these state contributions are equally balanced. In other words, there is equal probability to collapse the device state upon measurement to one that favors the  $S_1$  exchange coupling or to one that favors some sort of anisotropy (magnetic or between  $S_2$  and  $S_3$ ).

Similarly by turning off the exchange coupling between  $S_1$  and the two  $S_{2,3}$  particles, the  $x$ -axis rotation is suppressed, leading to rotation solely about the  $z$ -axis with frequency  $D + \Delta_{23}$ . Combinations of these rotations, accomplished by appropriate tuning of  $J_1$ , can realize any point on the Bloch sphere. By turning off these interactions, or utilizing another type of anisotropy (e.g., if one can control  $\Delta_{23}$ ), the dynamics can be stopped after a desired rotation operation after a given time  $t$ . Thus any relevant operation in the qubit representation on the Bloch sphere, and by extension any equivalent  $SU(2)$  operation, can be accomplished by utilizing the  $D$ - $J$  resonance.

Next, we find that when small values of anisotropy of the exchange coupling are included, the numerical calculation of the Bloch vector's projection on the  $x$ -axis oscillates, resulting in a correspondingly small deviation in its  $z$ -axis projection. This originates from the inclusion of additional off-diagonal states [e.g., see Eq. (7)] that correspond with one of the azimuthal axes in the Bloch sphere. Moreover, these additional states include contributions of the exchange interaction between particles 2 and 3, so that five parameters now control the rotation of the Bloch vector. Despite these contributions, we find that for certain parameters, the projection of the Bloch vector onto the  $z$ -axis (which directly corresponds with the switching behavior as measured by the electron) results in a

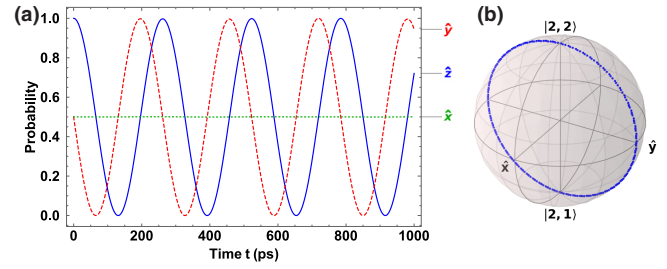


FIG. 3. (a) Probability of measuring a state corresponding with the  $\hat{x}$  (dotted),  $\hat{y}$  (dashed), and  $\hat{z}$  (solid) unit vectors on the Bloch sphere defined in Fig. 2, as a function of time. The Bloch vector is initially prepared in the state  $|\downarrow\rangle|2, 2\rangle$ , and an anisotropic application of the exchange coupling strength has been used ( $\Delta_1/J_1 = 0.072$ ). The parameter set has been prepared around the  $D$ - $J$  resonance. (b) The corresponding Bloch sphere representation of the path traced by the Bloch vector over the same time interval considered. In units of  $\text{cm}^{-1}$ , the parameters are  $J_{23} = -0.05$ ,  $J_1 = -0.40$ ,  $D = -0.60$ ,  $t = 0.05$ .

maximal transition probability above  $P = 0.995$  even when using significant ratios of anisotropy in the application of the exchange coupling, in our case  $\Delta_1/J_1 = 0.072$ , as shown in Fig. 3. When the anisotropic application of the exchange coupling is larger than the  $\Delta_1/J_1 = 0.072$  ratio for the set of parameters considered, the projection onto the Bloch sphere's  $z$ -axis is more distorted, as additional rotations about axes lying in the azimuthal plane are included.

We also find that there doesn't appear to be a simple relationship of the distortions and the strength of  $J_{23}$ . For example, using the same parameters as Fig. 3 and setting  $J_{23} = 0.60 \text{ cm}^{-1}$ , we find that the maximal transition probability remains above  $P = 0.995$ . When  $J_{23} = -0.20 \text{ cm}^{-1}$ , the maximal transition probability falls below  $P = 0.995$ , but again rises above  $P = 0.995$  when  $J_{23} = -0.40 \text{ cm}^{-1}$ . The  $\Delta_{23}$  parameter, on the other hand, provides a target from which to maintain fidelity. Inspection of the  $D$ - $J$  resonance conditions indicate that modulating  $J_1$  to account for  $\Delta_{23}$  allows one to reach resonance. By looking to the variables that participate in the dynamics in each block of the Hamiltonian [e.g., Eq. (7)], we find that these distortions of the Rabi-like oscillations are enhanced by larger values of  $J_{xy}$  and  $\Delta_1$ , and thus the relative magnitudes of the five parameters ( $\Sigma_1$ ,  $\Delta_1$ ,  $J_{xy}$ ,  $\Delta_{23}$ , and  $D$ ) dictate the limit of robustness of a particular resonance scenario.

The behavior of the  $S_{2,3} = 1$  model is not possible for  $S_{2,3} = \frac{1}{2}$  without additional spin selection methods. Repeating the same type of procedure and analysis for the  $S_{2,3} = \frac{1}{2}$  model, and noting that magnetic anisotropy is not expected for  $S = \frac{1}{2}$  particles, we find that the maximum probability amplitude is  $8/9$  for both transition types. When the two states involved in a transition are mapped onto a Bloch sphere, the effect of the unitary operator as a rotation is not about an axis solely on the azimuthal plane, but instead contains a component in the polar plane.

#### IV. DISCUSSION

Figure 3 forms the primary consequence of the main result of this paper, namely, that resonance conditions exist in the

$S_{2,3} = 1$  model in which preparation and measurement of the coupled particles' degree of entanglement can be accomplished by appropriate measurement of the  $S_1 = \frac{1}{2}$  particle. Furthermore, realization of these  $D$ - $J$  resonances is robust against anisotropy of the exchange coupling between the coupled particles. This is found to not be the case for the  $S_{2,3} = \frac{1}{2}$  model. In particular, as shown in Table I, the  $D$ - $J$  resonance conditions for maximal transitions between nonentangled and entangled states are controlled by the nontrivial interaction of the exchange coupling,  $J_{12}$  and  $J_{13}$ , between particles 1 and 2 and 3, the anisotropic exchange coupling interaction  $\Delta_{23}$ , and the magnetic anisotropy  $D$  of particles 2 and 3 in the  $S_{2,3} = 1$  paradigm.

The  $D$ - $J$  resonance conditions indicate a possible avenue for investigating complex spin spaces and the conditions required to simplify complicated spin Hamiltonians, such as those that represent the interactions of magnetic monomers or dimers with an electron, or when applied to three-particle Bose-Hubbard-like spin models such as in ultracold optical lattices. It is interesting to note that because our model has not required particular physical mechanisms for the exchange coupling and magnetic anisotropy, it is possible that outside of condensed matter physics, the block diagonalization of similar  $\mathbb{C}^{18}$  state systems could result in isolated  $SO(2)$  representation subgroups. The  $D$ - $J$  resonance feature introduces a different level of control in Bloch vector rotation operations. The inclusion of the  $S_1 = \frac{1}{2}$  particle allows for preparation, manipulation, and reading of the entangled coupled particles.

In quantum dot QIS systems, states are often prepared with applied magnetic fields. Electrically controlled methods, however, are attractive because of the relative ease of manipulating electric fields within a variety of environmental conditions. The results of our model predict that single-electron control of entangled particles without any use of applied magnetic fields is possible. Furthermore, an important conclusion to be drawn from Fig. 3 is that the Bloch vector, in time, is forgiving against misalignment, so that this scheme does not actually require impossible experimental perfection to work.

Last, we note that if the resonances are used for QIS applications, several additional factors must be incorporated

that have not been considered in this paper. As an illustrative example, the parameters chosen in Fig. 3 are inspired by a scenario involving  $[Mn_3]_2$  [33]. The  $[Mn_3]_2$  dimer, however, has higher spin, and thus a formula to determine the resonance conditions for higher  $S_{2,3}$  is desired. For general QIS scenarios, the order of parameters used in Fig. 3 implies that several oscillations have completed within 1 ns. This time is smaller than relevant spin-lattice and spin-spin relaxation times in most novel molecular magnets and quantum dots. Tuning the magnitudes of the  $D$ ,  $\Delta_{23}$ , and  $J_1$  parameters can lead to faster oscillations. In this way one can identify the  $T_1$  and  $T_2$  times for a particular system and tailor the search of  $D$ - $J$  resonance conditions based on those parameters.

Determining a more complete picture of a transient  $S_1$  particle requires the incorporation of additional degrees of freedom not considered here, such as the  $S_1$  particle's source and drain. We note, however, that while the source of the  $S_1$  particle has not been explicitly identified, some generalizations of the source (e.g., to a conduction band of a metal) will not substantially change the overall model or results. On the other hand, if the  $S_1$  particle is not transient, but instead is confined on a surface or within bulk material, additional exchange coupling interactions between the particle and the confinement source may need to be accounted for. Regardless of the physical mechanism chosen to realize this model, the use of these  $D$ - $J$  resonances provides an exciting avenue to uncover interesting highly correlated spin phenomena.

## ACKNOWLEDGMENTS

We thank James Freericks, Peter Dowben, Volodymyr Turkowski, Silas Hoffman, Marisol Alcántara Ortigoza, and Dave Austin for helpful discussions. This work was supported by the Center for Molecular Magnetic Quantum Materials, an Energy Frontier Research Center funded by the U.S. Department of Energy, Office of Science, Basic Energy Sciences under Grant No. DESC0019330. The authors declare no competing financial interests.

- 
- [1] M. A. Nielsen and I. L. Chuang, *Quantum Computation and Quantum Information: 10th Anniversary Edition* (Cambridge University Press, Cambridge, 2010).
  - [2] D. Loss and D. P. DiVincenzo, *Phys. Rev. A* **57**, 120 (1998).
  - [3] J. R. Petta, A. C. Johnson, J. M. Taylor, E. A. Laird, A. Yacoby, M. D. Lukin, C. M. Marcus, M. P. Hanson, and A. C. Gossard, *Science* **309**, 2180 (2005).
  - [4] R. Hanson, L. P. Kouwenhoven, J. R. Petta, S. Tarucha, and L. M. K. Vandersypen, *Rev. Mod. Phys.* **79**, 1217 (2007).
  - [5] A. Noiri, J. Yoneda, T. Nakajima, T. Otsuka, M. R. Delbecq, K. Takeda, S. Amaha, G. Allison, A. Ludwig, A. D. Wieck, and S. Tarucha, *Appl. Phys. Lett.* **108**, 153101 (2016).
  - [6] A. Noiri, T. Nakajima, J. Yoneda, M. R. Delbecq, P. Stano, T. Otsuka, K. Takeda, S. Amaha, G. Allison, K. Kawasaki, Y. Kojima, A. Ludwig, A. D. Wieck, D. Loss, and S. Tarucha, *Nat. Commun.* **9**, 5066 (2018).
  - [7] T. Nakajima, A. Noiri, J. Yoneda, M. R. Delbecq, P. Stano, T. Otsuka, K. Takeda, S. Amaha, G. Allison, K. Kawasaki, A. Ludwig, A. D. Wieck, D. Loss, and S. Tarucha, *Nat. Nanotechnol.* **14**, 555 (2019).
  - [8] C. H. Yang, R. C. C. Leon, J. C. C. Hwang, A. Saraiva, T. Tanttu, W. Huang, J. Camirand Lemyre, K. W. Chan, K. Y. Tan, F. E. Hudson, K. M. Itoh, A. Morello, M. Pioro-Ladrière, A. Laucht, and A. S. Dzurak, *Nature (London)* **580**, 350 (2020).
  - [9] R. C. C. Leon, C. H. Yang, J. C. C. Hwang, J. C. Lemyre, T. Tanttu, W. Huang, K. W. Chan, K. Y. Tan, F. E. Hudson, K. M. Itoh, A. Morello, A. Laucht, M. Pioro-Ladrière, A. Saraiva, and A. S. Dzurak, *Nat. Commun.* **11**, 797 (2020).
  - [10] M. N. Leuenberger and D. Loss, *Nature (London)* **410**, 789 (2001).
  - [11] L. M. K. Vandersypen, M. Steffen, G. Breyta, C. S. Yannoni, M. H. Sherwood, and I. L. Chuang, *Nature (London)* **414**, 883 (2001).

- [12] R. Vincent, S. Klyatskaya, M. Ruben, W. Wernsdorfer, and F. Balestro, *Nature (London)* **488**, 357 (2012).
- [13] M. Ganzhorn, S. Klyatskaya, M. Ruben, and W. Wernsdorfer, *Nat. Nanotechnol.* **8**, 165 (2013).
- [14] M. Urdampilleta, S. Klyatskaya, M. Ruben, and W. Wernsdorfer, *Phys. Rev. B* **87**, 195412 (2013).
- [15] S. Thiele, F. Balestro, R. Ballou, S. Klyatskaya, M. Ruben, and W. Wernsdorfer, *Science* **344**, 1135 (2014).
- [16] K. S. Pedersen, A.-M. Ariciu, S. McAdams, H. Weihe, J. Bendix, F. Tuna, and S. Piligkos, *J. Am. Chem. Soc.* **138**, 5801 (2016).
- [17] K. Najafi, A. L. Wysocki, K. Park, S. E. Economou, and E. Barnes, *J. Phys. Chem. Lett.* **10**, 7347 (2019).
- [18] L. Bogani and W. Wernsdorfer, *Nat. Mater.* **7**, 179 (2008).
- [19] S. M. Cronenwett, T. H. Oosterkamp, and L. P. Kouwenhoven, *Science* **281**, 540 (1998).
- [20] M. N. Leuenberger and E. R. Mucciolo, *Phys. Rev. Lett.* **97**, 126601 (2006).
- [21] G. González, M. N. Leuenberger, and E. R. Mucciolo, *Phys. Rev. B* **78**, 054445 (2008).
- [22] J. Kondo, *Prog. Theor. Phys.* **32**, 37 (1964).
- [23] P. W. Anderson, *Phys. Rev.* **124**, 41 (1961).
- [24] R. Žitko, R. Peters, and T. Pruschke, *Phys. Rev. B* **78**, 224404 (2008).
- [25] S. Mehl and D. P. DiVincenzo, *Phys. Rev. B* **92**, 115448 (2015).
- [26] A. T. Costa, S. Bose, and Y. Omar, *Phys. Rev. Lett.* **96**, 230501 (2006).
- [27] F. Ciccarello, G. M. Palma, M. Zarccone, Y. Omar, and V. R. Vieira, *New J. Phys.* **8**, 214 (2006).
- [28] F. Ciccarello, G. Massimo Palma, M. Paternostro, M. Zarccone, and Y. Omar, *Solid State Sci.* **11**, 931 (2009).
- [29] R. Hiraoka, E. Minamitani, R. Arafune, N. Tsukahara, S. Watanabe, M. Kawai, and N. Takagi, *Nat. Commun.* **8**, 16012 (2017).
- [30] W. C. Chung, J. de Hond, J. Xiang, E. Cruz-Colón, and W. Ketterle, *Phys. Rev. Lett.* **126**, 163203 (2021).
- [31] S. Hill, R. S. Edwards, N. Aliaga-Alcalde, and G. Christou, *Science* **302**, 1015 (2003).
- [32] D. Gatteschi and R. Sessoli, *Angew. Chem. Int. Ed.* **42**, 268 (2003).
- [33] J.-X. Yu, G. Christou, and H.-P. Cheng, *J. Phys. Chem. C* **124**, 14768 (2020).